◆ Human Brain Mapping 36:695–706 (2015) ◆

Reduced $CMRO_2$ and Cerebrovascular Reserve in Patients With Severe Intracranial Arterial Stenosis: A Combined Multiparametric qBOLD Oxygenation and BOLD fMRI Study

Julien Bouvier,[1,2,3] Olivier Detante,[1,2,4] Florence Tahon,[5] Arnaud Attye,[5] Thomas Perret,[1,2] David Chechin,[3] Marianne Barbieux,[1,2,4] Kamel Boubagra,[5] Katia Garambois,[4] Irène Tropres,[2,6] Sylvie Grand,[1,2,5] Emmanuel L. Barbier,[1,2] and Alexandre Krainik[1,2,5]*

[1]*Inserm, U836, Grenoble, France*
[2]*Université Grenoble Alpes, Grenoble Institute of Neurosciences, Grenoble, France*
[3]*Philips France (Healthcare Activity), Suresnes, France*
[4]*Stroke Unit, Department of Neurology, Grenoble University Hospital, Grenoble, France*
[5]*Department of Neuroradiology and MRI, Grenoble University Hospital, Grenoble, France*
[6]*IRMaGe Facility, UJF – INSERM US17 – CNRS UMS 3552, Grenoble, France*

Abstract: Multiparametric quantitative blood oxygenation level dependent (mqBOLD) magnetic resonance Imaging (MRI) approach allows mapping tissular oxygen saturation (StO_2) and cerebral metabolic rate of oxygen ($CMRO_2$). To identify hemodynamic alteration related to severe intracranial arterial stenosis (SIAS), functional MRI of cerebrovascular reserve (CVR BOLD fMRI) to hypercapnia has been proposed. Diffusion imaging suggests chronic low grade ischemia in patients with impaired CVR. The aim of the present study was to evaluate how oxygen parameters (StO_2 and $CMRO_2$), assessed with mqBOLD approach, correlate with CVR in patients ($n = 12$) with SIAS and without arterial occlusion. The perfusion (dynamic susceptibility contrast), oxygenation, and CVR were compared. The MRI protocol conducted at 3T lasted approximately 1 h. Regions of interest measures on maps were delineated on segmented gray matter (GM) of middle cerebral artery territories. We have shown that decreased CVR is spatially associated with decreased $CMRO_2$ in GM of patients with SIAS. Further, the degree of ipsilateral CVR reduction was well-correlated with the amplitude of the $CMRO_2$ deficit. The altered $CMRO_2$ suggests the presence of a moderate ischemia explained by both a decrease in perfusion and in CVR. CVR and mqBOLD method may be helpful in the selection of patients with SIAS to advocate for medical therapy or percutaneous transluminal angioplasty-stenting. *Hum Brain Mapp 36:695–706, 2015.*

Key words: brain; intracranial arterial stenosis; stroke; BOLD fMRI; cerebrovascular reserve; hypercapnia; perfusion; microvasculature; tissular oxygen saturation (StO_2); cerebral metabolic rate of oxygen ($CMRO_2$)

Contract grant sponsor: Philips Healthcare [CIFRE Stipend (to J.B.)].

*Correspondence to: Alexandre Krainik; MRI Unit, Department of Neuroradiology and MRI, CS 10217, University Hospital of Grenoble, 38043 Grenoble Cedex 9, France.
E-mail: akrainik@chu-grenoble.fr

Received for publication 24 March 2014; Revised 23 September 2014; Accepted 1 October 2014.
DOI: 10.1002/hbm.22657
Published online 12 October 2014 in Wiley Online Library (wileyonlinelibrary.com).

INTRODUCTION

Steno-occlusive disease of the intracranial arteries leads to ischemic stroke which is the leading cause of disability [Lloyd-Jones et al., 2009]. At 2 years, the recurrence rate of ischemic event in the territory of the stenotic artery reaches up to 40%, and even 60% in case of clinical signs of hemodynamic disorders [Mazighi et al., 2006]. In case of severe intracranial arterial stenosis (SIAS), treatment management remains under debate. In case of recurrence of ischemic events such as stroke or transient ischemic attack and despite intensive medical treatment, percutaneous transluminal angioplasty and stenting (PTAS) have been proposed but the risk-benefit balance of PTAS is unclear due to its rate of morbidity [Chimowitz et al., 2011; Fiorella et al., 2007]. Thus, to better identify among patients those at higher risk of recurrence of ischemic events and to demonstrate post-therapeutic benefit, functional MRI of cerebral vasoreactivity (CVR) has been proposed to map the vascular reserve downstream the stenosis before and after treatment [Attye et al., 2014; Haller et al., 2008; Han et al., 2011; Heyn et al., 2010; Mandell et al., 2008].

Additionally, subtle abnormalities on diffusion imaging of the parenchyma with impaired CVR suggested the presence of low-grade ischemic injury [Conklin et al., 2011]. Indeed, previous studies using nuclear medicine imaging showed that patients have impaired CVR and oxygen metabolism when collateral supply was inadequate to maintain normal cerebral perfusion pressure [Baron and Jones, 2012; Nemoto et al., 2003]. These gold standard techniques are used to quantify relevant physiological variables.

Recent advances in brain oxygenation mapping using MRI would be of great interest to characterize noninvasively and to monitor vascular and metabolism disorders in patients with SIAS. Several BOLD MRI techniques have been proposed to map oxygen extraction fraction (OEF) in the clinical setting [An and Lin, 2000; Jensen-Kondering and Baron, 2012]. One of the most accurate, clinically applicable, approaches is based on the theoretical model (quantitative BOLD model) proposed by Yablonskiy and Haacke [He and Yablonskiy, 2007; Yablonskiy and Haacke, 1994]. Christen et al. have recently proposed a simple multiparametric qBOLD (mqBOLD) MR method, validated in rodents [Christen et al., 2011, 2014] and using numerical simulations [Christen et al., 2012c], to map (1) the tissular oxygen saturation (StO_2) which represents the ratio of oxyhemoglobin to total hemoglobin and (2) the cerebral metabolic rate of oxygen ($CMRO_2$). They showed the need for additional measurements such as cerebral blood volume (CBV) or T_2 to obtain reliable information on oxygenation with BOLD MRI [Christen et al., 2012a]. First results obtained with this model are very encouraging especially in the case of acute ischemic stroke [Bouvier et al., 2013; Christen et al., 2014].

Although CVR and oxygen metabolism have already been evaluated by TEP in patients with SIAS, no combined CVR and oxygenation mapping using MRI has yet been performed. Here, we used MRI to simultaneously evaluate brain oxygenation assessed with mqBOLD approach and CVR in patients with SIAS.

SUBJECTS AND METHODS

Study Participants

Patients were recruited in the Neurology Department of Grenoble University Hospital Inclusion criteria were: (1) SIAS of intracranial carotid artery or middle cerebral artery (MCA) diagnosed on CT angiography (stenosis >70% [Nguyen-Huynh et al., 2008; Samuels et al., 2000] without arterial occlusion); (2) no contra-indication to MRI scanning; (3) no contraindication to Gd-Dota intravenous administration; (4) no other evolutive disease such as respiratory, renal or cardiac insufficiencies, cancer, psychiatric disorder; (5) written informed consent obtained. Exclusion criteria were: (1) incomplete imaging in MR acquisition; (2) excessive head motion (translation or rotation > 2 mm or $> 2^\circ$ in any direction, respectively; (3) inappropriate hypercapnic stimulus; (4) active smoking 2 h prior MRI examination. The study was approved by the Grenoble University Hospital Ethics Committee (B120620-10).

MRI Protocol

MRI protocol (Fig. 1) was carried out on a 3T Achieva MR scanner (Philips Healthcare®), at the Grenoble University Hospital, using a whole-body RF transmit and eight-channel head receive coils. The total duration of the MR protocol was approximately 1 h.

Anatomical studies

Anatomical studies consisted of:

An axial T_2 Fluid Attenuated Inversion Recovery (FLAIR-WI) sequence (30 slices, thickness = 4 mm, TR/TE: 11,000/125 ms, 512 × 512 matrix, a field of view (FOV) of 230 × 180 mm, and 2.9 min acquisition time).

A three-dimensional (3D) gradient recalled echo (GRE) T_1-weighted image (WI) (160 contiguous slices, slice thickness = 1 mm, TR/TE: 9.8/4.6 ms, 512 × 512 matrix, a FOV of 256 × 160 mm, and 4.5 min acquisition time).

An intracranial MR angiography performed using a time of flight (TOF) sequence (130 slices, thickness = 1.4 mm, TR/TE: 25/3.4 ms, 560 × 560 matrix, a FOV of 220 × 180 mm, and 5.3 min acquisition time).

These sequences were acquired in an axial plane, parallel to the anterior commissure-posterior commissure, and covering the entire brain.

BOLD study for cerebral vasoreactivity

BOLD imaging consisted of a T_2^* WI GRE Echo Planar Imaging (EPI) acquisition (32 axial slices, slice

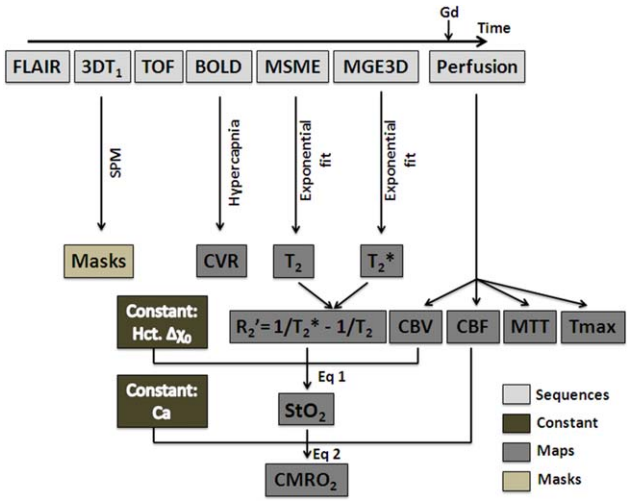

Figure 1.

Diagram of the acquisition and processing schemes to obtain CVR, perfusion, and oxygenation maps. FLAIR, fluid attenuated inversion recovery; TOF, time of flight; BOLD, blood oxygen level dependent; MSME, multi spin-echo; MGE3D, 3D multi gradient echo; SPM, statistical parametric mapping; CVR, cerebral vasoreactivity; CBV, cerebral blood volume; CBF, cerebral blood flow; MTT, mean transit time; Tmax, time-to-maximum; StO_2, tissular oxygen saturation; $CMRO_2$, cerebral metabolic rate of oxygen; Gd, gadolinium-DOTA; Hct, hematocrit; $\Delta\chi_0$, change in magnetic susceptibility between oxy and deoxyhemoglobin; Ca, arterial oxygen content. CBV and CBF are obtained from the basal perfusion study. StO_2 is derived from R'_2 and CBV. $CMRO_2$ is derived from StO_2 and CBF. CVR is an independent estimate.

thickness = 4 mm, TR/TE: 3,000/35 ms, alpha: 90°, 64 × 64 matrix, a FOV of 256 × 256 mm, and 12.1 min acquisition time) with a whole brain coverage.

The hypercapnic stimulus was block-designed using a gas mixture of 8% CO_2, 21% O_2, and 71% N_2. It was administered on simple blind mode with a high concentration mask according to the following paradigm: [air (1 min) − hypercapnia (2 min) − air (1 min)] × 3. Physiological parameters including end-tidal CO_2 pressure ($PetCO_2$), arterial oxygen saturation (SpO_2), breath frequency, and heart rate were monitored using a MR compatible device (Maglife, Schiller medical). This protocol induces an increase in $EtCO_2$ and partial pressure ($PetCO_2$) of about 10 mm Hg (Fig. 2), which was recorded via nasal canula.

Oxygenation study (mqBOLD)

Oxygenation study consisted of two sequences acquired in the same plane as the BOLD imaging, covering a 2-cm thick slab centerd on the lesion as previously detected by the TOF sequence:

A 3D multi gradient echo (MGE3D) sequence to obtain T_2^* estimates (25 slices, 23 echoes, TR/TE = 164/5.83 ms, ΔTE = 7 ms, 224 × 224 matrix, resolution = 1 × 1 × 0.8 mm, and 4.23 min acquisition time);

A multi spin-echo (MSME) to map T_2 (5 slices, TR/TE = 1,282/9 ms, 32 echoes, ΔTE = 9.04 ms, 112 × 112 matrix, resolution = 2 × 2 × 4 mm, and 3.07 min acquisition time).

Basal perfusion study

In addition to the oxygenation sequences, perfusion-WI MRI (PWI) was performed by dynamic gradient-echo echo-planar imaging (25 contiguous slices, thickness = 4 mm, TR/TE: 1,670/40 ms, 112 × 112 matrix, a FOV of 224 × 184 mm), tracking a bolus of 0.1 mmol/kg of Gadolinium-DOTA (0.1 mmol/kg, Guerbet, France), injected at a rate of 5 mL/s with a magnetic resonance compatible power injector (MEDRAD, Warrendale, PA). This injection was flushed with a bolus of physiological saline (60 mL). An injection delay of 10 s was applied to obtain an accurate estimate of the baseline MR signal intensity S(0) prior to the arrival of the contrast agent. Eighty single-shot, gradient-echo, echo-planar images, were obtained in each of the slices during the 1.08 min acquisition time.

Data Processing and Analysis

Data analysis was performed using MATLAB (MathWorks, Natick, MA), the SPM8 software (SPM, Wellcome Department of Imaging Neuroscience, http://www.fil.ion.ucl.ac.uk/spm/), and custom routines.

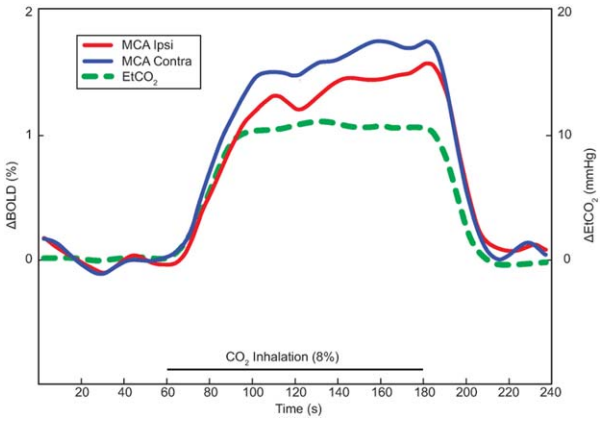

Figure 2.

Regressor used for fMRI analyses based on mean $EtCO_2$ variation time courses during hypercapnia (green line). Percentage of BOLD signal averaged over three blocks. Mean BOLD signal time courses of MCA territories ipsilateral and contralateral to the SIAS were represented by red and blue lines, respectively. Both amplitude and initial slope of the BOLD time course decreased in the MCA territory ipsilateral to the SIAS.

Anatomical data

Gray and white matters (GM and WM) were segmented through the 3D GRE T_1 sequence, and a GM mask was obtained by thresholding the individually smoothed GM maps. T_2-FLAIR was analyzed to rate the microangiopathy according to the simplified Fazekas scale [Inzitari et al., 2009].

BOLD data

Preprocessing steps included in-plane motion correction (realignment), spatial normalization to the Montreal Neurologic Institute (MNI) T_1-weighted template, and spatial smoothing with a 16-mm Gaussian Kernel.

BOLD CVR fMRI was acquired with a block-design hypercapnic challenge (8% CO_2). The averaged end-tidal CO_2 pressure ($EtCO_2$) across all patient and corrected for a 4.8-s delay was used as a physiological regressor for statistical analyses with a general linear model (SPM8) (Fig. 2). The averaged regressor was used for all subjects without individual timing adjustment. CVR was expressed as percent change of BOLD signal per mm Hg change of $PetCO_2$.

Perfusion data

The arterial input function was extracted from a single slice of the perfusion scan containing the MCA. Next, the mean transit time (MTT), and the time-to-maximum (Tmax) maps were calculated pixel-wise with a deconvolution approach. This approach was based on a singular value decomposition [Ostergaard et al., 1996] using a tracer arrival timing insensitive method and an automatic regularization of oscillations (oSVD) [Wu et al., 2003].

The relative cerebral blood volume (rCBV) was estimated from the area under the curve of the voxel concentration. To obtain quantitative maps, the mean brain CBV was normalized to 5%. The MTT and Tmax maps were estimated from the area under the curve and from the time to maximum of the deconvolved function, respectively [Meier and Zierler, 1954]. rCBF was calculated as the ratio rCBV/MTT from the central volume theorem [Stewart, 1893]. The excluded voxels from the computation were averaged with the nearby voxels.

Oxygenation data

The mqBOLD data were processed as described in [Christen et al., 2011] and illustrated on Figure 1. Briefly, StO_2 maps were obtained pixelwise from a combination of CBV and T'_2 according to the following equation:

$$StO_2 = 1 - (4/3 \cdot \pi \cdot \gamma \cdot B_0 \cdot \Delta\chi_0 \cdot Hct \cdot T'_2 \cdot CBV)^{-1}. \quad (1)$$

where $1/T'_2 = 1/T_2^* - 1/T_2$, $\Delta\chi_0 = 0.264 \times 10^{-6}$ is the difference in magnetic susceptibilities between fully oxygenated and fully deoxygenated hemoglobin, Hct = 0.42 is the hematocrit fraction, $\gamma = 2.675 \times 10^8$ rad/s/**T** is the nuclear gyromagnetic ratio, and $B_0 = 3$T is the strength of the main magnetic field. T_2 and T_2^* maps were calculated by fitting a monoexponential decay to the corresponding MR images. To correct for macroscopic magnetic field inhomogeneities, the 3D gradient echo sequence was spatially averaged [Christen et al., 2011]. The final spatial resolution was that of the multi spin-echo sequence: $2 \times 2 \times 4$ mm. Numerical simulations demonstrated that the contribution of the intravascular signal may be neglected in the mqBOLD approach [Christen et al., 2012b].

Eventually, the $CMRO_2$ was computed pixel-wise using:

$$CMRO_2 = CaO_2 \times CBF \times (SaO_2 - StO_2) \quad (2)$$

where SaO_2, the arterial oxygen saturation and CaO_2, the arterial oxygen content, were set to 100% and 19 mL O_2/100 mL of blood, respectively [An et al., 2001; West, 2007].

Finally, StO_2, $CMRO_2$, and perfusion maps were coregistered to the T_2 map and normalized to the MNI T_1-weighted template using BOLD imaging matrix transformation. After normalization, the final spatial resolution was $2 \times 2 \times 2$ mm.

Thus, maps of basal perfusion, oxygenation, and vasoreactivity maps were obtained for each subject.

Regions of interest (ROI) measures on both %BOLD signal change/mm Hg $EtCO_2$ and others maps were delineated on segmented GM of the vascular territories [Tatu et al., 2012]. We calculated mean values and laterality indices (LI) in MCA territories for each parameter (CBF, CBV, MTT, Tmax, CVR, StO_2, and $CMRO_2$), $LI_{MCA} = (Left\_Value_{MCA} - Right\_Value_{MCA})/(Left\_Value_{MCA} + Right\_Value_{MCA})$.

Statistical analysis

Statistical analyses were conducted using SPSS 18.0®. Kolmogorov–Smirnov tests on variables of interest (CBV, CBF, MTT, Tmax, CVR, $CMRO_2$, and StO_2) and associated LI showed no significant differences to normal distribution. Subsequently, parametric statistical studies were performed. Interhemispheric comparisons for mean ROI_{MCA} values were estimated using paired Student's *t*-test. Correlations studies across parameters were estimated using the *R* Pearson coefficient. To examine the ability of perfusion and CVR to predict $CMRO_2$, we conducted linear regression studies with stepwise backward selection. The exit value in the logistic regression was set at 0.10. Adjusted odds ratios were calculated with 95% confidence intervals. Statistical significance was set for $P < 0.05$. All data are expressed as mean ± standard deviation (m ± sd).

RESULTS

Seventeen patients were enrolled into the study. No adverse reaction to the Gd-dota administration and to hypercapnic stimulus was reported. Five patients were

TABLE I. Patient characteristics

Patient	SIAS location	Age (yo)	Gender	Symptoms	Degree of stenosis (%)	Active smoking	Hypertension	Dyslipidemia	Diabetes
1	Right ICA	75	F	Monoparesia of the left superior limb	73	N	Y	Y	N
2	Right ICA	66	M	Transient left hemiparesia	70	Y	N	N	N
3	Right ICA	75	M	Transient monoparesia of the left superior limb	72	Y	N	Y	N
4	Left ICA	81	M	None	77	N	Y	Y	N
5	Left ICA	59	M	Recurrent transient monoparesia of the left superior limb	79	Y	N	Y	N
6	Right and left MCA	67	M	None	Right: 71 Left: 70	N	Y	Y	N
7	Right MCA	65	M	Transient left hemiparesia	74	N	Y	N	Y
8	Right MCA	85	F	Transient left hemiparesia	72	N	Y	Y	N
9	Right MCA	59	M	Recurrent transient monoparesia of the left superior limb	71	N	N	N	N
10	Right MCA	53	M	None	70	N	N	N	N
11	Left MCA	62	M	Transient aphasia	71	Y	Y	Y	N
12	Left MCA	28	M	Recurrent transient right hemiparesia	80	Y	N	Y	N

Abbreviations: SIAS, severe intracranial arterial stenosis; ICA, internal carotid artery; MCA, middle cerebral artery; yo, years old; F, female; M, male; Y, yes; N, no.

excluded because of incomplete protocol realization secondary to discomfort due to the face mask within the head coil ($n = 2$), inappropriate hypercapnic stimulus because the manual change of gas inhalation did not follow the predefined paradigm ($n = 1$), or excessive movements that were not due to the hypercapnic stimulus ($n = 2$), leaving 12 patients for further analyses (10 men, 2 women; age range from 28 to 85 years old (64.6 ± 14.9 years old). Indeed, no patient reported significant side effect that might have led to interrupt the hypercapnic stimulus and the MR examination.

SIAS of the anterior circulation were located on the right intracranial internal carotid (ICA) ($n = 3$), the left ICA ($n = 2$), the right MCA ($n = 5$), or the left MCA ($n = 3$). One patient ($n°6$) had severe stenosis of both left and right MCA. For this subject, we arbitrarily chose to define the right MCA territory as ipsilateral to the stenosis. The percentage of stenosis ranged from 70 to 80%. We did not find arterial stenosis $> 50\%$ on extracranial internal carotid artery, anterior, and posterior cerebral arteries. Nine patients had anterior SIAS-related symptoms. Patients' characteristics are summarized in Table I.

TABLE II. Patient laterality indices

Patient	SIAS location	LI_{MCA} CBF	LI_{MCA} Tmax	LI_{MCA} MTT	LI_{MCA} CVR	LI_{MCA} $CMRO_2$	LI_{MCA} StO_2
1	Right ICA	0.11	0.04	−0.01	0.04	0.07	0.05
2	Right ICA	0.06	−0.06	−0.04	0.12	0.06	−0.02
3	Right ICA	0.05	−0.13	−0.07	0.06	0.06	−0.04
4	Left ICA	0.05	−0.13	−0.16	−0.01	−0.01	−0.06
5	Left ICA	−0.15	0.22	0.10	−0.1	−0.06	−0.12
6	Right and left MCA	−0.04	−0.18	−0.05	−0.1	−0.05	−0.05
7	Right MCA	0.08	−0.08	−0.03	0.04	0.04	0.03
8	Right MCA	0.13	−0.01	−0.07	0.13	0.11	−0.05
9	Right MCA	0.07	−0.05	−0.01	0.1	0.03	0.00
10	Right MCA	0.08	0.02	−0.01	0.14	0.05	0.02
11	Left MCA	−0.12	0.18	0.05	−0.02	−0.09	−0.08
12	Left MCA	−0.16	0.22	0.16	−0.27	−0.18	0.05

Abbreviations: ICA, internal carotid artery; MCA, middle cerebral artery; LI, laterality indices; SIAS, severe intracranial arterial stenosis; CBF, cerebral blood flow; Tmax, time-to-maximum; MTT, mean transit time; CVR, cerebrovascular reserve; $CMRO_2$, cerebral metabolic rate of oxygen; StO_2, tissular oxygen saturation.

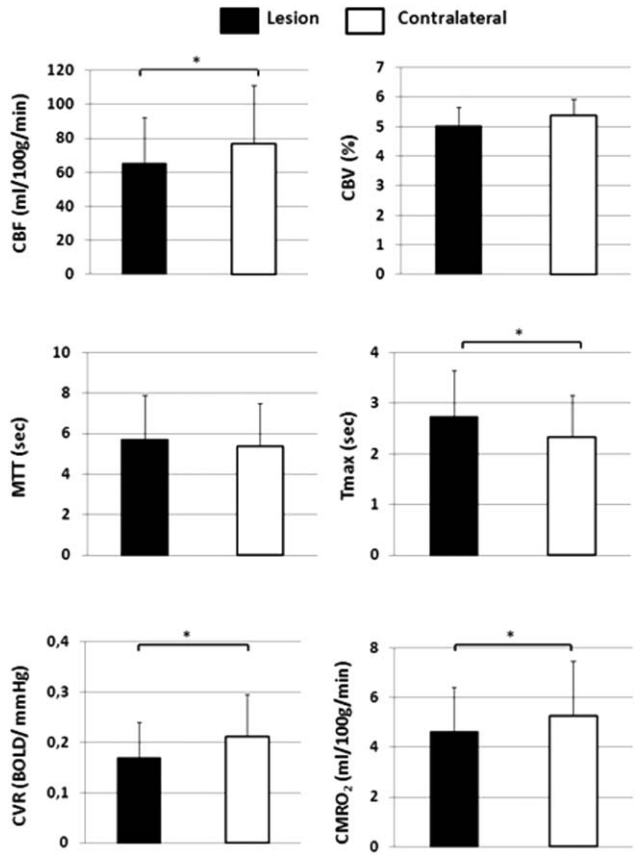

Figure 3.
(**a**) CBF, (**b**) CBV, (**c**) MTT, (**d**) Tmax, (**e**) CVR, and (**f**) $CMRO_2$ obtained from the SIAS ipsilateral and the contralateral MCA territories and averaged across patients ($n = 12$) (mean ± SD).

Basal Perfusion

In the SIAS ipsilateral MCA territory compared to contralateral MCA territory, we observed a decrease of CBF (65.2 ± 27.2 vs. 76.6 ± 34.5 mL/100 g/min; $P < 0.01$) and an increase of Tmax (2.7 ± 0.9 vs. 2.3 ± 0.8 s; $P < 0.04$). Their interhemispheric differences estimated using lateral indices ranged for LI_{MCA}_CBF from −0.16 to 0.13 and for LI_{MCA}_Tmax from −0.18 to 0.22 (Table II). No difference was observed for CBV or MTT (respectively: 5.0 ± 0.6 vs. 5.4 ± 0.6% and 5.7 ± 2.2 vs. 5.4 ± 2.1 s) (Fig. 3a–d).

Cerebral Vasoreactivity

BOLD signal curves obtained after normalization for the $EtCO_2$ time lag and regressor used for fMRI analyses based on mean $EtCO_2$ variation time courses during hypercapnia are represented in Figure 2.

Mean CVR values were lower in the SIAS ipsilateral MCA territory than in the contralateral (0.18 ± 0.07 vs. 0.21 ± 0.08 %BOLD/mm Hg, $P < 0.01$) (Fig. 3e). LI_{MCA}_CVR values ranged from −0.27 to 0.14.

Oxygenation

Mean $CMRO_2$ values in the SIAS ipsilateral MCA territory were significantly lower than in the contralateral (4.2 ± 1.8 vs. 4.8 ± 2.2 mL/100 g/min, $P < 0.02$) (Fig. 3f).

For mean StO_2 values, no difference was observed between the SIAS ipsilateral MCA territory and the contralateral territory (45.2 ± 5.1 vs. 46.4 ± 5.4%). LI_{MCA}_$CMRO_2$ values ranged from −0.18 to 0.11 and LI_{MCA}_StO_2 from −0.12 to 0.05.

Correlations and Regression Studies

Correlation analyses were conducted to investigate the relationships between basal perfusion, CVR, and oxygenation mapping.

In the SIAS ipsilateral hemisphere, $CMRO_2$ was positively correlated with CBF ($R = 0.96$, $P < 0.001$), and negatively correlated with MTT ($R = -0.78$, $P < 0.003$) and Tmax ($R = -0.59$; $P < 0.04$). No correlation was observed with CBV ($R = -0.12$), StO_2 ($R = -0.025$) or CVR ($R = 0.06$). No correlation was detected between StO_2 and CVR or between basal perfusion parameters and CVR.

In the contralateral hemisphere, $CMRO_2$ was positively correlated with CBF ($R = 0.96$, $P < 0.001$), and negatively correlated with MTT ($R = -0.74$, $P < 0.006$) and Tmax ($R = -0.59$; $P < 0.04$). No correlation was observed with CBV ($R = 0.23$), StO_2 ($R = 0.21$), or CVR ($R = 0.12$). No correlation was detected between StO_2 and CVR or between basal perfusion parameters and CVR.

For interhemispheric differences estimated by LI, we found positive correlations between LI_{MCA}_$CMRO_2$ and LI_{MCA}_CBF ($R = 0.93$; $P < 0.001$) (Fig. 4a), LI_{MCA}_CVR ($R = 0.92$; $P < 0.001$) (Fig. 4b), and LI_{MCA}_MTT ($R = -0.68$; $P < 0.02$). A trend toward a negative correlation was found between LI_{MCA}_$CMRO_2$ and LI_{MCA}_Tmax ($R = -0.57$; $P < 0.06$). LI_{MCA}_CVR also correlated with LI_{MCA}_CBF ($R = 0.84$; $P < 0.001$) and LI_{MCA}_MTT ($R = -0.61$; $P < 0.04$).

Illustrative cases are shown in Figure 5.

DISCUSSION

We report the first MR study in patients with SIAS combining measurements of basal perfusion, CVR using BOLD imaging during hypercapnic challenge, and tissular oxygenation using mqBOLD. In such patients, a previous study suggested that low-grade ischemia may occur in the parenchyma downstream [Conklin et al., 2011]. Indeed, in this vascular territory, we detected strong correlations between oxygenation ($CMRO_2$) and CVR impairments (Fig. 4). These results are in line with previous works using PET or DTI, and show strong relationships between the disorders of basal and functional change in perfusion and oxygen metabolism due to SIAS.

mqBOLD Approach: A Promising MR Technique

A previous study reported decreased T'_2 values in regions with perfusion delay presumably reflecting focally

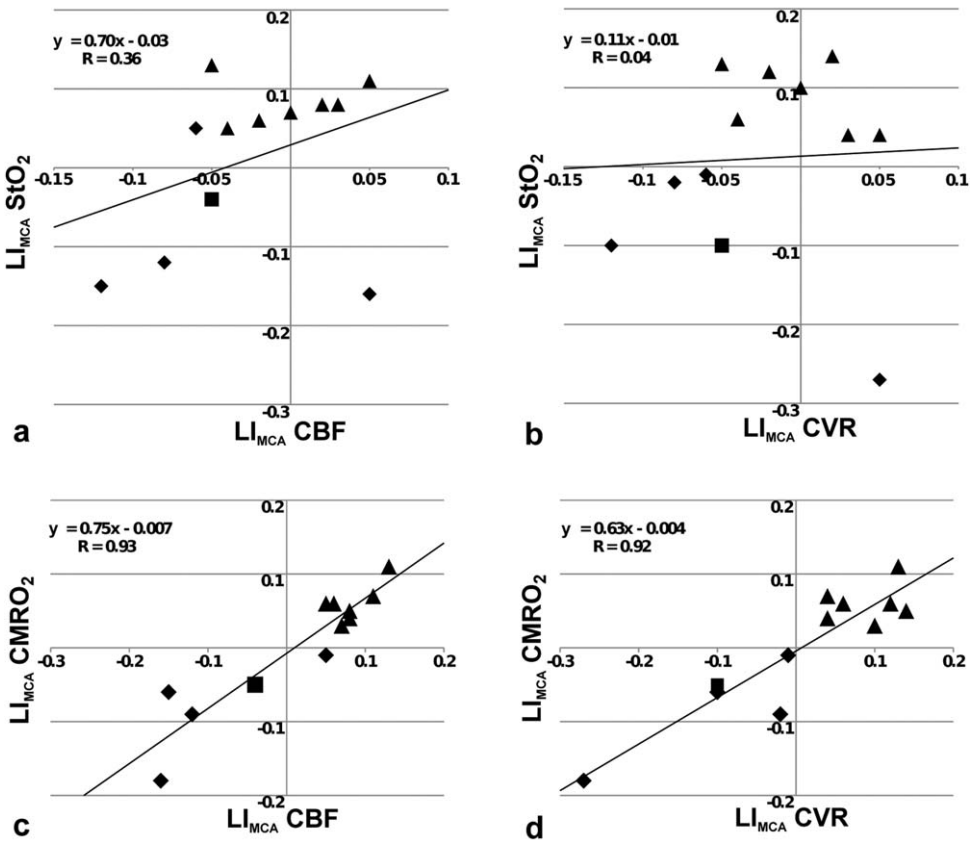

Figure 4.

(**a**) $LI_{MCA}\_StO_2$ versus LI_{MCA}_CBF, (**b**) $LI_{MCA}\_StO_2$ versus LI_{MCA}_CVR, (**c**) $LI_{MCA}\_CMRO_2$ versus LI_{MCA}_CBF, and (**d**) $LI_{MCA}\_CMRO_2$ versus LI_{MCA}_CVR ($n = 12$). StO_2, tissular oxygen saturation; CBF, cerebral blood flow; $CMRO_2$, cerebral metabolic rate of oxygen; CVR, cerebrovascular reserve; LI_{MCA}, laterality indices in MCA territories. Each triangle, diamond and square represents patient with right (MCA/ICA), Left (MCA/ICA) or bilateral (MCA/ICA) stenosis, respectively.

increased OEF, but did not directly correlate this modification with CVR [Seiler et al., 2012]. Another recent investigation showed a significant OEF increase in the hemisphere ipsilateral to the stenotic or occluded artery compared with the contralateral hemisphere [Xie et al., 2011], which is consistent with others studies [Grubb et al., 1998; Hokari et al., 2008]. However, to our knowledge, the present study is the first study by MRI to combine oxygenation mapping with perfusion and CVR imaging in patients with SIAS. Although, the correlation between $CMRO_2$ and CVR was not statistically significant quantitatively, we suppose that a similar relationship may exist in other pathologies that cause chronic CVR impairment: for example, in patients with Alzheimer's disease [Cantin et al., 2011; Fukuyama et al., 1994].

Basal Perfusion and Oxygenation Values

It has already been shown by PET that there are regional differences in $CMRO_2$ and CBF in normal subjects at rest. Indeed, CBF and $CMRO_2$ are always high in the visual cortex and seem to be accompanied by a low OEF in the sensorimotor cortex [Ishii et al., 1996]. Our method provides parametric maps with sufficient spatial resolution to distinguish regional differences in the contralateral hemisphere (Fig. 5). However, with our approach, $CMRO_2$ and CBF are partially dependent [Eq. (2)].

A previous report by MRI showed that in patients with severe atherosclerotic MCA disease, OEF increased when CBF decreased [Xie et al., 2011]. Actually, significant OEF increase was detected when CBF decreased below 50% in the affected MCA territory when compared to the opposite side. In our study, a decreased CBF was observed in the hemisphere ipsilateral to the vascular lesion (Fig. 3), which is consistent with hemodynamic impairment [Derdeyn et al., 1999]. This CBF decreases remained mild with a maximal |LI_CBF| of 0.16. Taken together with the absence of interhemispheric StO_2 difference, it suggests that OEF remained stable in the affected hemisphere. Thus, when considering that OEF was stable, the $CMRO_2$ decrease could be mainly related to the CBF drop.

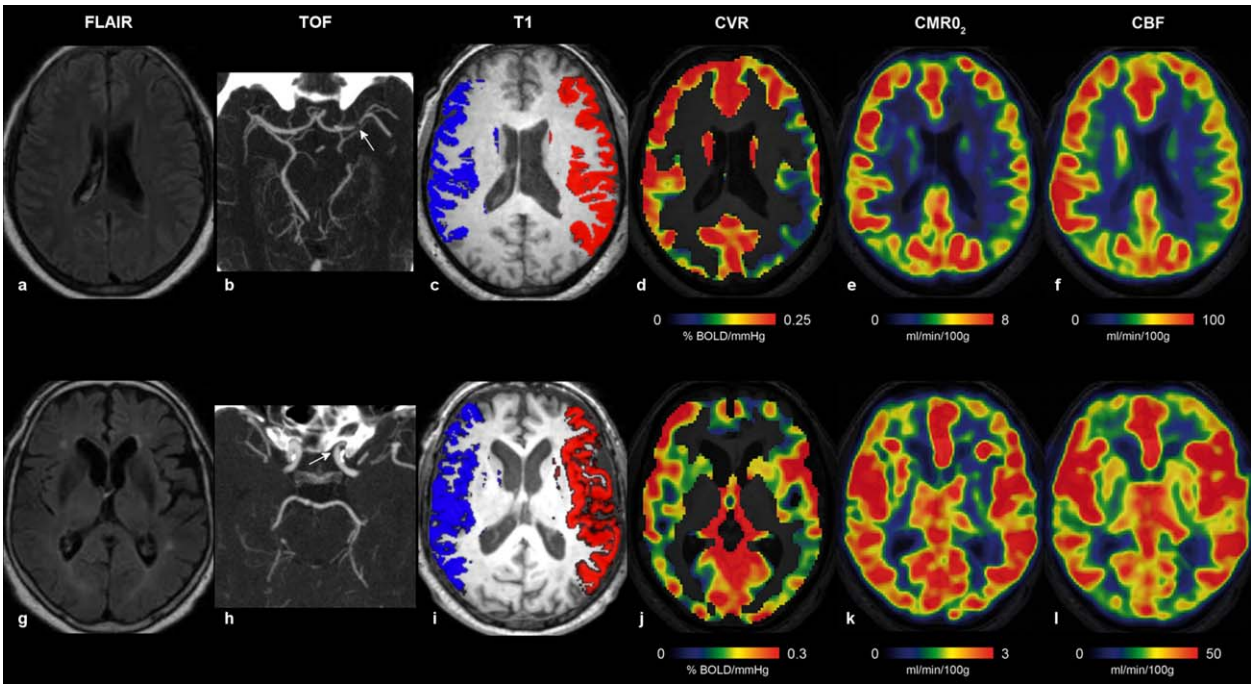

Figure 5.

Illustrative individual maps of Patient #12 (upper row, a–f) and Patient #4 (lower row, g–l), representing FLAIR (a, g), TOF with stenosis (white arrows) (b, h), ROIs used for delineate the MCA territories overlaid onto axial T_1-WI (c, i), BOLD response to hypercapnia (d, j), $CMRO_2$ (e, k), and CBF (f, l). Patient #12 had a combined reduction of CBF, CVR, and $CMRO_2$ in the left MCA territory downstream a left MCA SIAS, whereas Patient #4 with a left ICA SIAS had symmetrical values.

CVR and Oxygenation Values

OEF measured by PET and CVR to acetazolamide have been used as predictors for subsequent ischemic stroke in patients with occlusive carotid artery diseases [Kuroda et al., 2001; Ogasawara et al., 2002]. However, recent studies have shown that reduced CVR is not always accompanied by an elevated OEF. Indeed, Kuroda et al. and Nemoto et al [Yamauchi et al., 1999] showed that only half of the patients with reduced CVR also had an elevated OEF.

Here, we could not measure OEF directly. However, while StO_2 was not asymmetrically decreased in the ipsilateral hemisphere despite reduced perfusion and CVR, OEF could be regionally maintained. Nevertheless, this compensation seemed to be insufficient to avoid a $CMRO_2$ decrease. These results may correspond to a hemodynamic compromise. In the Powers' classification revised by Nemoto et al. for chronic stage [Nemoto et al., 2004], decreased perfusion, oxygenation, and CVR correspond to stage IIIc. However, individual data reveal different status. Patient 6 exhibited a slight predominance of abnormalities in the left hemisphere despite of a bilateral and symmetrical SIAS. Patient 4 had symmetrical CVR and $CMRO_2$ with LIs close to 0. Indeed, 5 patients out of 12 had a weaker asymmetry with CVR $|LI| < 0.1$. Actually, normal ranges of perfusion, oxygenation, and CVR asymmetries are missing in the literature, and ought to be defined in normal population. However, in our experience of CVR BOLD fMRI in 100 controls, 95% of this population had CVR $|LI| < 0.08$. In patients with unilateral severe MCA stenosis, about 40% had abnormal values (unpublished data). It is likely that the severity of asymmetry is related to the risk of recurrence of stroke event but thresholds have to be defined to better adjust treatment strategy. For instance, we report the case of a patient with symptomatic severe MCA stenosis despite aggressive medical treatment, who required percutaneous stenting. In this patient, CVR BOLD fMRI accounted for a decrease of vascular reserve of 31.6%, corresponding to a CVR $|LI|$ of 0.19 [Attye et al., 2014]. Thus, in clinical practice and especially in patients with SIAS, individual analyses are relevant to discuss treatment strategy. Significant CVR impairment is inconstant, and among these patients, the level of CVR impairment that may further justify arterial stenting remains to be defined. Oxygenation mapping could be useful to better identify those patients.

We agree that absolute quantification of perfusion, oxygenation, and CVR is the ultimate goal. However, even with absolute values, abnormal values have to be defined,

and among these thresholds have to be identified with a therapeutic perspective. Because of methodological limitations, absolute quantification of these parameters using MRI is not entirely established yet. Then, we advocate that such semiquantitative approach could be helpful to better discuss therapeutic care in asymmetrical diseases such as unilateral SIAS.

Regarding quantitative function MRI, it has been proposed that R'_2 could be used as a measure of the maximum BOLD signal [Blockley et al., 2012]. However, it our hands neither R'_2 nor StO_2 was correlated to CVR (absolute values or laterality index, data not shown).

Oxygenation and CVR Limitations

Important distortions and signal drops were detected in the fronto-basal and temporo-basal regions especially on EPI sequences. However, they were out of the ROI that were drawn into the midpart of the MCA territories and should not affect the results presented in this study.

The values of StO_2 in our study were consistent with those of PET studies reported and relatively lower than those of MRI study [Xie et al., 2011]. Consequently, $CMRO_2$ values appeared slightly higher than those of PET [Tanaka et al., 2008]. To obtain a quantitative measurement of oxygenation, one must have a known hematocrit and quantitative CBV. A more accurate oxygenation measurement could be obtained using a local microvascular Hct value for each voxel. Such estimate is not available and we therefore choose to use a systemic Hct value. This Hct value may yields an absolute, positive, bias on the StO_2 estimates obtained in this study. This global bias does not however impact the reported correlations. To improve the evaluation of CBV, one could use a steady-state approach and iron oxide particles [Christen et al., in press]. Indeed, this approach is not limited by acquisition time and a sufficient signal to noise ratio can be obtained to create CBV maps with up to 1 mm^3 isotropic spatial resolution. The excellent accuracy on CBV estimates obtained with this approach may be worth the use of additional contrast. Alternatively to the total CBV measurement, methods have been proposed to measure venous blood volume only [Bulte et al., 2007; Stefanovic and Pike, 2005]. The use of these methods could provide an estimate of SvO_2 (the venous oxygen saturation) instead of StO_2 (the tissue oxygen saturation, i.e., the average blood oxygen saturation across the arterio-venous network). In this study, intravascular effects were not included in our model [Christen et al., 2012b]. However, it has been reported elsewhere that the contribution of intravascular signal should not be neglected [He and Yablonskiy, 2007]. This point requires additional studies.

Similarly, an average $EtCO_2$ was used as a physiological regressor instead of an individual $EtCO_2$. In fact, BOLD responses could depend on vasomotor differences due to any variability in the capnic modulation across patients and not only to the presence of the disease [Cantin et al., 2011]. Indeed, individual $EtCO_2$ regressor may account for interindividual differences at the whole brain CVR level expressed in %BOLD/mm Hg. However, subtle $EtCO_2$ differences across subjects could hardly account for significant intraindividual differences such as those expected when comparing homologous interhemispheric values. Note that the hypercapnic stimulus used is a safe, well-tolerated, and technically applicable in clinical patient population [Krainik et al., 2013; Spano et al., 2013]. The stimulus was achieved with our block-designed paradigm and a 2-min hypercapnic exposure to provide sufficient perfusion increase to perform BOLD CVR imaging. No patient reported significant side effect that might have led to interrupt the hypercapnic stimulus and the MR examination.

The small sample size is another limitation of study. Nonparametric tests such as Spearman's correlation confirmed all the results, especially the relationships between $LI_{MCA}\_CMRO_2$ and LI_{MCA}_CBF, and $LI_{MCA}\_CMRO_2$ and LI_{MCA}_CVR represented onto the Figure 4. However, Spearman's correlations failed to reach significance for the following correlations: (1) between $CMRO_2$ and Tmax in the SIAS ipsilateral hemisphere ($rho = -0.38$; $P < 0.23$); (2) between $LI_{MCA}\_CMRO_2$ and LI_{MCA}_MTT ($rho = -0.55$; $P < 0.06$); (3) between $LI_{MCA}\_CMRO_2$ and LI_{MCA}_Tmax ($rho = 0.30$; $P < 0.35$); (4) between LI_{MCA}_CVR and LI_{MCA}_MTT ($rho = -0.40$; $P < 0.2$). We might expect that these correlations between $CMRO_2$ or BOLD CVR with temporal parameters of basal perfusion would be confirmed in a larger sample. Although statistical parameters and tests provide precious information in large population samples, odd results remain informative. They might reveal biases or even subtle differences across individuals that might have not been taken into account during the population selection, the data analysis, and interpretation given to the scientific knowledge at the time of the study. In fact, we previously illustrated this phenomenon using fMRI in brain-lesioned patients referred for stroke [Krainik et al., 2005] and tumors [Jiang et al., 2010]. Although interhemispheric changes were commonly interpreted as cortical reorganization and neuronal plasticity, we have shown that these changes were correlated to CVR impairment, suggesting that a vascular disorder may explain a significant proportion of fMRI activation variance. These results raised the limitations of the use of a biophysical model in complex and partially understood functional imaging in non-canonical population, as suggested by our previous works and by [Blicher et al., 2012].

Here, we show the relationships between $CMRO_2$, basal perfusion, and CVR using MRI. Despite these relationships, we could not explain why some patients, such as Patient 11, are far from the regression lines. Moreover, several patients harbored significant interhemispheric asymmetry, we suspect those $|LI| > 0.10$, others did not. Now, we can hardly explain with our dataset why, among patients with similar SIAS, some have reduced CVR and $CMRO_2$ and others do not. However, this information could be helpful to better choose treatment strategy.

Low-Grade Ischemic Injury

The global and regional variations in the CVR observed in patients may be related to modifications in the basal cerebral perfusion, consistent with a previous report [Ogasawara et al., 2002]. In this study, CVR impairment was also associated with a decreased $CMRO_2$ in GM of patients with SIAS. The altered $CMRO_2$ suggests the presence of a moderate ischemia explained by both a decrease in perfusion and in CVR. Indeed, it has been shown that CVR impairment was associated with increased ADC in the normally appearing WM of patients with SIAS, which may represent low-grade ischemic injury [Conklin et al., 2011].

Here, mqBOLD results may reinforce this hypothesis. Combined with CVR fMRI that may help to predict the risk of hemodynamic stroke due to SIAS, this imaging of "at risk" downstream brain tissue in SIAS could provide useful additional data, beyond stenosis degree and clinical signs, to better select patients and advocate for endovascular angioplasty-stenting. The medical or endovascular therapy for SIAS is still debated however; new selection parameters could be added for further clinical trials to assess and to follow tissue oxygenation and microvascular adaptations.

CONCLUSION

This study is the first report of $CMRO_2$ obtained with MRI on patients with SIAS disease. The metabolism alteration was related to a decrease in vasoreactivity capacity and a hemodynamic impairment, which also supports the presence of low-grade ischemia previously suggested by diffusion imaging. The mqBOLD method provided high resolution maps in patients with SIAS and may be a promising complementary MRI technique in the management of patients with hemodynamic disorders. This approach may be helpful for a better selection of patients to undergo endovascular angioplasty-stenting or medical therapy to prevent ischemic stroke.

ACKNOWLEDGMENTS

The authors acknowledge the help of the MRI facility of Grenoble (UMS IRMaGe) for their experimental support. The authors acknowledge the precious help of Mrs. Nicole Triplett-Rupin for editing the manuscript.

REFERENCES

An H, Lin W (2000): Quantitative measurements of cerebral blood oxygen saturation using magnetic resonance imaging. J Cereb Blood Flow Metab 20:1225–1236.

An H, Lin W, Celik A, Lee YZ (2001): Quantitative measurements of cerebral metabolic rate of oxygen utilization using MRI: A volunteer study. NMR Biomed 14:441–447.

Attye A, Villien M, Tahon F, Warnking J, Detante O, Krainik A (2014): Normalization of cerebral vasoreactivity using BOLD MRI after intravascular stenting. Hum Brain Mapp 35:1320–1324.

Baron JC, Jones T (2012): Oxygen metabolism, oxygen extraction and positron emission tomography: Historical perspective and impact on basic and clinical neuroscience. NeuroImage 61:492–504.

Blicher JU, Stagg CJ, O'Shea J, Ostergaard L, MacIntosh BJ, Johansen-Berg H, Jezzard P, Donahue MJ (2012): Visualization of altered neurovascular coupling in chronic stroke patients using multimodal functional MRI. J Cerebral Blood Flow Metab 32:2044–2054.

Blockley NP, Griffeth VE, Buxton RB (2012): A general analysis of calibrated BOLD methodology for measuring CMRO2 responses: Comparison of a new approach with existing methods. NeuroImage 60:279–289.

Bouvier J, Detante O, Tropres I, Grand S, Chechin D, Le Bas J-F, Krainik A, Barbier EL (2013): Evaluation of a multiparamteric qBOLD approach in acute stroke patients. ISMRM. Salt Lake City, Etats-Unis.

Bulte D, Chiarelli P, Wise R, Jezzard P (2007): Measurement of cerebral blood volume in humans using hyperoxic MRI contrast. J Magn Reson Imaging 26:894–899.

Cantin S, Villien M, Moreaud O, Tropres I, Keignart S, Chipon E, Le Bas JF, Warnking J, Krainik A (2011): Impaired cerebral vasoreactivity to CO_2 in Alzheimer's disease using BOLD fMRI. NeuroImage 58:579–587.

Chimowitz MI, Lynn MJ, Derdeyn CP, Turan TN, Fiorella D, Lane BF, Janis LS, Lutsep HL, Barnwell SL, Waters MF, Hoh BL, Hourihane JM, Levy EI, Alexandrov AV, Harrigan MR, Chiu D, Klucznik RP, Clark JM, McDougall CG, Johnson MD, Pride GL Jr, Torbey MT, Zaidat OO, Rumboldt Z, Cloft HJ, SAMMPRIS Trial Investigators (2011): Stenting versus aggressive medical therapy for intracranial arterial stenosis. N Engl J Med 365:993–1003.

Christen T, Lemasson B, Pannetier N, Farion R, Segebarth C, Remy C, Barbier EL (2011): Evaluation of a quantitative blood oxygenation level-dependent (qBOLD) approach to map local blood oxygen saturation. NMR Biomed 24:393–403.

Christen T, Lemasson B, Pannetier N, Farion R, Remy C, Zaharchuk G, Barbier EL (2012a): Is T2* enough to assess oxygenation? Quantitative blood oxygen level-dependent analysis in brain tumor. Radiology 262:495–502.

Christen T, Schmiedeskamp H, Straka M, Bammer R, Zaharchuk G (2012b): Measuring brain oxygenation in humans using a multiparametric quantitative blood oxygenation level dependent MRI approach. Magn Reson Med 68:905–911.

Christen T, Zaharchuk G, Pannetier N, Serduc R, Joudiou N, Vial JC, Remy C, Barbier EL (2012c): Quantitative MR estimates of blood oxygenation based on T2*: A numerical study of the impact of model assumptions. Magn Reson Med 67:1458–1468.

Christen T, Bouzat P, Pannetier N, Coquery N, Moisan A, Lemasson B, Thomas S, Grillon E, Detante O, Remy C, Payen JF, Barbier EL (2014): Tissue oxygen saturation mapping with magnetic resonance imaging. J Cereb Blood Flow Metab 34:1550–1557.

Christen T, Ni W, Qiu D, Schmiedeskamp H, Bammer R, Moseley M, Zaharchuk G: High-resolution cerebral blood volume imaging in humans using the blood pool contrast agent ferumoxytol. Magn Reson Med. 2012 Sep 21. doi: 10.1002/mrm.24500. [Epub ahead of print]

Conklin J, Fierstra J, Crawley AP, Han JS, Poublanc J, Silver FL, Tymianski M, Fisher JA, Mandell DM, Mikulis DJ (2011):

Mapping white matter diffusion and cerebrovascular reactivity in carotid occlusive disease. Neurology 77:431–438.

Derdeyn CP, Grubb RL Jr, Powers WJ (1999): Cerebral hemodynamic impairment: Methods of measurement and association with stroke risk. Neurology 53:251–259.

Fiorella D, Levy EI, Turk AS, Albuquerque FC, Niemann DB, Aagaard-Kienitz B, Hanel RA, Woo H, Rasmussen PA, Hopkins LN, Masaryk TJ, McDougall CG (2007): US multicenter experience with the wingspan stent system for the treatment of intracranial atheromatous disease: Periprocedural results. Stroke 38:881–887.

Fukuyama H, Ogawa M, Yamauchi H, Yamaguchi S, Kimura J, Yonekura Y, Konishi J (1994): Altered cerebral energy metabolism in Alzheimer's disease: A PET study. J Nucl Med 35:1–6.

Grubb RL Jr, Derdeyn CP, Fritsch SM, Carpenter DA, Yundt KD, Videen TO, Spitznagel EL, Powers WJ (1998): Importance of hemodynamic factors in the prognosis of symptomatic carotid occlusion. JAMA 280:1055–1060.

Haller S, Bonati LH, Rick J, Klarhofer M, Speck O, Lyrer PA, Bilecen D, Engelter ST, Wetzel SG (2008): Reduced cerebrovascular reserve at CO2 BOLD MR imaging is associated with increased risk of periinterventional ischemic lesions during carotid endarterectomy or stent placement: Preliminary results. Radiology 249:251–258.

Han JS, Abou-Hamden A, Mandell DM, Poublanc J, Crawley AP, Fisher JA, Mikulis DJ, Tymianski M (2011): Impact of extracranial-intracranial bypass on cerebrovascular reactivity and clinical outcome in patients with symptomatic moyamoya vasculopathy. Stroke 42:3047–3054.

He X, Yablonskiy DA (2007): Quantitative BOLD: Mapping of human cerebral deoxygenated blood volume and oxygen extraction fraction: Default state. Magn Reson Med 57:115–126.

Heyn C, Poublanc J, Crawley A, Mandell D, Han JS, Tymianski M, terBrugge K, Fisher JA, Mikulis DJ (2010): Quantification of cerebrovascular reactivity by blood oxygen level-dependent MR imaging and correlation with conventional angiography in patients with Moyamoya disease. Am J Neuroradiol 31:862–867.

Hokari M, Kuroda S, Shiga T, Nakayama N, Tamaki N, Iwasaki Y (2008): Combination of a mean transit time measurement with an acetazolamide test increases predictive power to identify elevated oxygen extraction fraction in occlusive carotid artery diseases. J Nucl Med 49:1922–1927.

Inzitari D, Pracucci G, Poggesi A, Carlucci G, Barkhof F, Chabriat H, Erkinjuntti T, Fazekas F, Ferro JM, Hennerici M, Langhorne P, O'Brien J, Scheltens P, Visser MC, Wahlund LO, Waldemar G, Wallin A, Pantoni L, LADIS Study Group (2009): Changes in white matter as determinant of global functional decline in older independent outpatients: Three year follow-up of LADIS (leukoaraiosis and disability) study cohort. BMJ 339:b2477.

Ishii K, Sasaki M, Kitagaki H, Sakamoto S, Yamaji S, Maeda K (1996): Regional difference in cerebral blood flow and oxidative metabolism in human cortex. J Nucl Med 37:1086–1088.

Jensen-Kondering U, Baron JC (2012): Oxygen imaging by MRI: Can blood oxygen level-dependent imaging depict the ischemic penumbra? Stroke 43:2264–2269.

Jiang Z, Krainik A, David O, Salon C, Tropres I, Hoffmann D, Pannetier N, Barbier EL, Bombin ER, Warnking J, Pasteris C, Chabardes S, Berger F, Grand S, Segebarth C, Gay E, Le Bas JF (2010): Impaired fMRI activation in patients with primary brain tumors. NeuroImage 52:538–548.

Krainik A, Hund-Georgiadis M, Zysset S, von Cramon DY (2005): Regional impairment of cerebrovascular reactivity and BOLD signal in adults after stroke. Stroke 36:1146–1152.

Krainik A, Villien M, Tropres I, Attye A, Lamalle L, Bouvier J, Pietras J, Grand S, Le Bas JF, Warnking J (2013): Functional imaging of cerebral perfusion. Diagn Interv Imaging 94:1259–1278.

Kuroda S, Houkin K, Kamiyama H, Mitsumori K, Iwasaki Y, Abe H (2001): Long-term prognosis of medically treated patients with internal carotid or middle cerebral artery occlusion: Can acetazolamide test predict it? Stroke 32:2110–2116.

Lloyd-Jones D, Adams R, Carnethon M, De Simone G, Ferguson TB, Flegal K, Ford E, Furie K, Go A, Greenlund K, Haase N, Hailpern S, Ho M, Howard V, Kissela B, Kittner S, Lackland D, Lisabeth L, Marelli A, McDermott M, Meigs J, Mozaffarian D, Nichol G, O'Donnell C, Roger V, Rosamond W, Sacco R, Sorlie P, Stafford R, Steinberger J, Thom T, Wasserthiel-Smoller S, Wong N, Wylie-Rosett J, Hong Y, American Heart Association Statistics Committee, Stroke Statistics Subcommittee (2009): Heart disease and stroke statistics–2009 update: A report from the American Heart Association Statistics Committee and Stroke Statistics Subcommittee. Circulation 119:480–486.

Mandell DM, Han JS, Poublanc J, Crawley AP, Stainsby JA, Fisher JA, Mikulis DJ (2008): Mapping cerebrovascular reactivity using blood oxygen level-dependent MRI in patients with arterial steno-occlusive disease: Comparison with arterial spin labeling MRI. Stroke 39:2021–2028.

Mazighi M, Tanasescu R, Ducrocq X, Vicaut E, Bracard S, Houdart E, Woimant F (2006): Prospective study of symptomatic atherothrombotic intracranial stenoses: The GESICA study. Neurology 66:1187–1191.

Meier P, Zierler KL (1954): On the theory of the indicator-dilution method for measurement of blood flow and volume. J Appl Physiol 6:731–744.

Nemoto EM, Yonas H, Chang Y (2003): Stages and thresholds of hemodynamic failure. Stroke 34:2–3.

Nemoto EM, Yonas H, Kuwabara H, Pindzola RR, Sashin D, Meltzer CC, Price JC, Chang Y, Johnson DW (2004): Identification of hemodynamic compromise by cerebrovascular reserve and oxygen extraction fraction in occlusive vascular disease. J Cereb Blood Flow Metab 24:1081–1089.

Nguyen-Huynh MN, Wintermark M, English J, Lam J, Vittinghoff E, Smith WS, Johnston SC (2008): How accurate is CT angiography in evaluating intracranial atherosclerotic disease? Stroke 39:1184–1188.

Ogasawara K, Ogawa A, Yoshimoto T (2002): Cerebrovascular reactivity to acetazolamide and outcome in patients with symptomatic internal carotid or middle cerebral artery occlusion: A xenon-133 single-photon emission computed tomography study. Stroke 33:1857–1862.

Ostergaard L, Weisskoff RM, Chesler DA, Gyldensted C, Rosen BR (1996): High resolution measurement of cerebral blood flow using intravascular tracer bolus passages. Part I: Mathematical approach and statistical analysis. Magn Reson Med 36:715–725.

Samuels OB, Joseph GJ, Lynn MJ, Smith HA, Chimowitz MI (2000): A standardized method for measuring intracranial arterial stenosis. Am J Neuroradiol 21:643–646.

Seiler A, Jurcoane A, Magerkurth J, Wagner M, Hattingen E, Deichmann R, Neumann-Haefelin T, Singer OC (2012): T2′ imaging within perfusion-restricted tissue in high-grade occlusive carotid disease. Stroke 43:1831–1836.

Spano VR, Mandell DM, Poublanc J, Sam K, Battisti-Charbonney A, Pucci O, Han JS, Crawley AP, Fisher JA, Mikulis DJ (2013): CO_2 blood oxygen level-dependent MR mapping of cerebrovascular reserve in a clinical population: Safety, tolerability, and technical feasibility. Radiology 266:592–598.

Stefanovic B, Pike GB (2005): Venous refocusing for volume estimation: VERVE functional magnetic resonance imaging. Magn Reson Med 53:339–347.

Stewart GN (1893): Researches on the circulation time in organs and on the influences which affect it: Parts I-III. J Physiol 15:1–89.

Tanaka M, Shimosegawa E, Kajimoto K, Kimura Y, Kato H, Oku N, Hori M, Kitagawa K, Hatazawa J (2008): Chronic middle cerebral artery occlusion: A hemodynamic and metabolic study with positron-emission tomography. Am J Neuroradiol 29: 1841–1846.

Tatu L, Moulin T, Vuillier F, Bogousslavsky J (2012): Arterial territories of the human brain. Front Neurol Neurosci 30:99–110.

West J (2007): Pulmonary Physiology and Pathophysiology: An Integrated, Case-Based Approach. Philadelphia, PA: Lippincott Williams & Wilkins.

Wu O, Ostergaard L, Weisskoff RM, Benner T, Rosen BR, Sorensen AG (2003): Tracer arrival timing-insensitive technique for estimating flow in MR perfusion-weighted imaging using singular value decomposition with a block-circulant deconvolution matrix. Magn Reson Med 50:164–174.

Xie S, Hui LH, Xiao JX, Zhang XD, Peng Q (2011): Detecting misery perfusion in unilateral steno-occlusive disease of the internal carotid artery or middle cerebral artery by MR imaging. Am J Neuroradiol 32:1504–1509.

Yablonskiy DA, Haacke EM (1994): Theory of NMR signal behavior in magnetically inhomogeneous tissues: The static dephasing regime. Magn Reson Med 32:749–763.

Yamauchi H, Fukuyama H, Nagahama Y, Nabatame H, Ueno M, Nishizawa S, Konishi J, Shio H (1999): Significance of increased oxygen extraction fraction in five-year prognosis of major cerebral arterial occlusive diseases. J Nucl Med 40:1992–1998.